Biophysical Chemistry 30 (1988) 49–59
Elsevier

BPC 01231

Frequency-domain measurements of the rotational dynamics of the tyrosine groups of calmodulin

I. Gryczynski [a,*], J.R. Lakowicz [a] and R.F. Steiner [b]

[a] *Department of Biological Chemistry, School of Medicine, University of Maryland at Baltimore, Baltimore, MD 21201 and* [b] *Department of Chemistry, University of Maryland, Catonsville, MA 21228, U.S.A.*

Received 1 September 1987
Revised version received 5 October 1987
Accepted 2 November 1987

Calmodulin; Tyrosine; Frequency-domain fluorometry; Fluorescence anisotropy decay; Fluorescence intensity decay

We used frequency-domain fluorometry to determine the intensity and anisotropy decay kinetics of tyrosine residues in calmodulin and its fragments. Excitation was provided by a continuous ultraviolet laser source, a frequency-doubled rhodamine 6G ring dye laser, whose output was externally modulated to 200 MHz. Both the intensity and anisotropy decays were found to be multiexponential and dependent upon temperature and solution conditions. By examination of calmodulin fragments we determined that energy transfer between the two tyrosine residues reduces the steady-state anisotropy values by about 20%. Additionally, the frequency-domain anisotropy decays indicate local torsional motions of the tyrosine residues, as well as significant individual motions of the two domains of calmodulin.

1. Introduction

Calmodulin, a Ca^{2+}-binding protein widely distributed in eukaryotic systems, has been demonstrated to be involved in the regulation of numerous enzymes [1,2]. Its interaction with a regulated enzyme is generally Ca^{2+}-dependent and involves interaction of the Ca^{2+}-liganded form of calmodulin with the enzyme [1,2]. The binding of Ca^{2+} by calmodulin has been shown to result in a major conformational change, which is reflected by an increase in α-helical content, a microenvironmental change of the two tyrosines, and the generation, or exposure, of hydrophobic sites of attachment for several ligands [1–3].

The crystallographic structure of calmodulin has recently been determined for Ca^{2+}-liganded calmodulin [4]. The molecule is dumbbell-shaped with an N-terminal and a C-terminal lobe joined by a connecting helical strand (residues 66–92). The molecule is 65 Å long; the dimensions of the two lobes are 20 × 20 × 25 Å. The crystallographic structure appears to be relatively rigid and asymmetric. It is uncertain to what extent it persists in solution.

The purpose of the present paper is to examine the molecular dynamics of calmodulin, as reflected by the rotational motion of its two tyrosines, employing the recently developed technique of frequency-domain fluorometry [5–9]. Both of the tyrosines, Tyr-99 and Tyr-138, are located within the C-terminal lobe and form part of Ca^{2+}-binding domains III and IV, respectively [4]. Rotational mobility of these residues can be mea-

Correspondence address: I. Gryczynski, Department of Biological Chemistry, School of Medicine, University of Maryland at Baltimore, Baltimore, MD 21201, U.S.A.

Abbreviations: Ac, acetate; Clm, calmodulin; GuHCl, guanidine hydrochloride; Mops, 3-(*N*-morpholino)-2-hydroxypropanesulfonic acid.

sured from the time-dependent anisotropy decays, which we obtain from the frequency response of the polarized emission [6]. Rotational motions of the tyrosine residues, relative to the overall structure, can reflect a rotation of the C-terminal lobe, a rotational wobble of the adjacent polypeptide, or a rotation of the phenolic side chain about its covalent bond. Additionally, the time-dependent anisotropy can decrease due to homotransfer between the two tyrosine residues, which is expected to occur with a Förster distance of 10–15 Å [10,11] which is comparable to the distance between the two tyrosine residues in calmodulin.

2. Materials and methods

Calmodulin was prepared from bovine testes (Pel-Freez) by a procedure based on that of Watterson, et al. [12]. The product was homogeneous when examined by SDS-acrylamide gel electrophoresis or acrylamide gel electrophoresis in 8 M urea.

The TR_2C fragment of calmodulin (residues 78–148) was prepared by trypsin digestion of calmodulin in the presence of excess Ca^{2+} according to the procedure of Brzeska et al. [13], followed by HPLC separation of the fragments, as described previously [14,15]. The initial digestion was carried to completion, as judged by acrylamide gel electrophoresis in 5 M urea. The TM_1 (residues 1–106) and TM_2 (residues 107–148) fragments of calmodulin were prepared by complete thrombin digestion in the absence of Ca^{2+}, followed by HPLC separation [14,15]. The homogeneity of all fragments was verified by acrylamide gel electrophoresis in 5 M urea and by amino acid analysis. The amino acid compositions corresponded closely to the expected values [13–15]. Amino acid analyses were performed by Dr. Lou Henderson. All chemicals were reagent grade or better. Glass-redistilled water was used for the preparation of all solutions.

3. Theory

Measurements were performed on a frequency-domain fluorometer which has been described in detail elsewhere [5]. This instrument was modified by addition of a 15 W argon ion laser, which pumps a Coherent 699 ring dye laser containing rhodamine 6G [16]. The wavelength of the dye laser was halved in a continuous manner to 285–300 nm using an angle-tuned KDP crystal placed within the laser cavity. This source provides about 0.5 mW of continuous ultraviolet at the excitation wavelength 285 nm. The ultraviolet output was modulated with a Lasermetrics 1042 electro-optic modulator. Phase and modulation data are typically obtained at 25 modulation frequencies spaced approximately equally on a logarithmic scale from 1 to 200 MHz. Intensity decays were measured using magic angle polarization conditions which eliminate the effects of rotational motions on the decay [17]. The frequency-dependent phase (ϕ_ω) and modulation (m_ω) values were fitted to a multiexponential decay law,

$$I(t) = \sum_i \alpha_i e^{-t/\tau_i} \tag{1}$$

as described previously [5,7]. In this expression α_i and τ_i are the amplitude and decay time, respectively, of the i-th component. The fractional intensity (f_i) of each component of the emission is given by

$$f_i = \alpha_i \tau_i / \sum \alpha_i \tau_i. \tag{2}$$

For anisotropy decay measurements the sample is excited with vertically polarized light which is intensity modulated. The measured values are the phase angle difference (Δ_ω) between the perpendicular ($\phi_\perp$) and parallel ($\phi_\parallel$) components of the modulated emission,

$$\Delta_\omega = \phi_\perp - \phi_\parallel \tag{3}$$

and the ratio of the amplitudes of the modulated emission (Λ_ω)

$$\Lambda_\omega = m_\parallel / m_\perp \tag{4}$$

The subscript ω refers to the modulation frequency (in rad/s). The modulated amplitude data are better understood by using the modulated anisotropy

$$r_\omega = \frac{\Lambda_\omega - 1}{\Lambda_\omega + 2} \tag{5}$$

This value is analogous to the steady-state anisotropy, except that it is dependent upon the modulation frequency. At low frequencies r_ω becomes equivalent to the steady-state anisotropy. At high frequencies it becomes equal to the fundamental anisotropy with no rotational diffusion (r_0). The frequency-domain data (Δ_ω and Λ_ω) are fitted to a time-dependent anisotropy ($r(t)$) decay

$$r(t) = r_0 \sum_i g_i e^{-t/\theta_i} \qquad (6)$$

where the θ_i are the correlation times, g_i the associated amplitudes, and r_0 the limiting anisotropy at zero time. In this report we used the known values of r_0, measured at low temperatures in vitrified solvents. Hence, the variable parameters in eq. 6 are θ_i and g_i, with the restriction that $\Sigma g_i = 1.0$.

The quality of fit is assessed by the value of reduced chi-squared (χ^2_R), which is the weighted sum of the squared deviations divided by the number of degrees of freedom (ν)

$$\chi^2_R = \frac{1}{\nu}\sum_\omega \left(\frac{\Delta_\omega - \Delta_{\omega c}}{\delta\Delta}\right)^2 + \frac{1}{\nu}\sum_\omega \left(\frac{\Lambda_\omega - \Lambda_{\omega c}}{\delta\Lambda}\right)^2 \qquad (7)$$

Here $\Delta_{\omega c}$ and $\Lambda_{\omega c}$ are the values computed using an assumed set of parameters characterizing the time decay of anisotropy according to eq. 6: $\delta\Delta$ and $\delta\Lambda$ are the errors for phase and modulation measurements, respectively. A similar procedure was used to analyze the intensity decay ($I(t)$) in terms of individual decay constants.

4. Results

4.1. Tyrosine intensity decays

The intensity decays of the intrinsic tyrosine emission from calmodulin were determined under a variety of experimental conditions (tables 1 and 2). In most cases an adequate fit was attained only with the assumption of two decay times, except in the absence of Ca^{2+} where the data support a three-decay-time model. This is illustrated in fig. 1, which shows data for the frequency-domain intensity decay at pH 6.5 and 5°C in the presence of 5 mM EGTA. The data are clearly not described by a single decay time, which is evident from the lack of agreement of the single-decay-time model (— — —) with the data (●) and the large and nonrandom deviation (○, lower panels). Failure of the single-decay-time model is also evident from the elevated value of $\chi^2_R = 685$. It was more difficult, but still possible, to reject the two-decay-time fit (●●●●). For this model $\chi^2_R = 2.5$. The three-component model yields random deviations and an acceptable value of $\chi^2_R = 1.21$. With our approx. 50 degrees of freedom a 2.1-fold elevation in χ^2_R occurs with a probability of less than 1%, which makes it unlikely that random errors in the data caused the elevation in χ^2_R. While the recovered amplitudes and decay times adequately represent the data, these parameters do not necessarily establish that three components are strictly present. The intensity decays may be the result of a distribution of decay times [18,19],

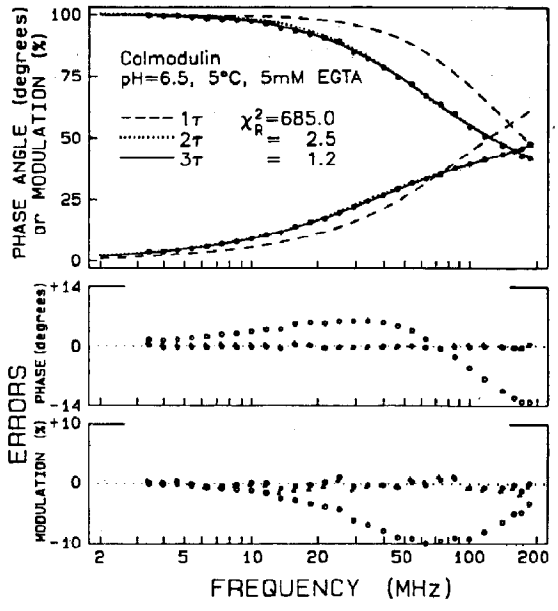

Fig. 1. Frequency-domain data for the intensity decay of calmodulin at pH 6.5 and 5°C, in the presence of 5 mM EGTA. (———) Three-component fit through the data (●). (------) Best single-decay-time fit. (·····) Best two-component fit. The lower panel shows the deviations for the best (○) one-, (▲) two- and (●) three-decay-time fits. The values of χ^2_R are 685, 2.53 and 1.21, respectively.

Table 1

Decay times for calmodulin tyrosine fluorescence (pH 6.5)

Conditions [a]	Temperature (° C)	τ_i (ns)	α_i	f_i	$\bar{\tau}$ (ns) [b]	χ_R^2
5 mM EGTA	5	0.621	0.794	0.389		
		3.756	0.206	0.611	2.536	2.53 [c]
		0.558	0.763	0.346		
		3.070	0.217	0.540		
		7.020	0.020	0.114	2.652	1.21
	37	0.560	0.804	0.445		
		2.859	0.196	0.555	1.836	2.54
		0.463	0.752	0.364		
		2.228	0.234	0.544		
		6.022	0.015	0.092	1.935	1.10
5 mM Ca^{2+}	5	1.862	0.704	0.466		
		5.071	0.296	0.534	3.576	1.56
		1.768	0.638	0.402		
		4.366	0.336	0.523		
		8.344	0.025	0.075	3.616	1.43
	37	1.149	0.713	0.420		
		3.938	0.287	0.580	2.910	1.66
		0.841	0.408	0.179		
		1.759	0.387	0.356		
		4.336	0.205	0.465	2.793	1.45
6 M GuHCl	25	0.945	0.682	0.410		
		2.918	0.318	0.590	2.109	1.59
		0.943	0.678	0.406		
		1.873	0.008	0.010		
		2.928	0.314	0.584	2.111	1.61

[a] All solutions contained 50 mM Mops (pH 6.5). The concentration of calmodulin was 94 μM, except for the solution with 6 M GuHCl, which was 100 μM.

[b] Calculated from $\Sigma_i f_i \tau_i$ with $\Sigma f_i = 1.0$

[c] For calculation of χ_R^2 the degrees of random error were assumed to be 0.2° of phase and 0.005 for the modulation.

which could have their origin in the composite nature of the emission and the dynamic properties of the protein on the nanosecond time scale. The emission corresponds to the summed contributions of two tyrosines, which may sample multiple microenvironments by varying orientations of the tyrosines.

The values of the individual decay times are dependent upon conditions. This is illustrated in fig. 2, which shows data for the same conditions as fig. 1, except for the presence of 5 mM Ca^{2+}. The presence of calcium results in an increase in the mean decay time, which is seen from a shift in the frequency response to lower frequencies, as compared with fig. 1. In the absence and presence of calcium the mean decay times, calculated using $\Sigma_i f_i \tau_i$, are 2.5 and 3.6 ns, respectively. The mean decay time was found to decrease with increasing temperature, in both the presence and absence of calcium. For instance, the mean decay times with 5 mM Ca^{2+} are 3.6 and 2.8 at 5 and 37°C, respectively.

We also examined the intensity decays at pH 5, under conditions which are nearly identical to those used for determination of the crystal structure [4]. Once again, the decays were found to be multiexponential, and at least two components were usually needed to account for the data (table 2). As was found at pH 6.5, the decay times increased with binding of calcium and decreased

Table 2

Decay times for calmodulin tyrosine fluorescence (pH 5.0 and 5 mM Ca^{2+})

Conditions [a]	Temperature (°C)	τ_i (ns)	α_i	f_i	$\bar{\tau}$ (ns)	χ_R^2
33 μM	5	1.682	0.686	0.449		
		4.509	0.314	0.551	3.239	2.27
		1.547	0.592	0.358		
		3.731	0.373	0.544		
		7.133	0.035	0.097	3.276	2.24
	25	1.380	0.763	0.533		
		3.885	0.237	0.467	2.550	1.37
		1.212	0.604	0.374		
		2.732	0.349	0.486		
		5.848	0.047	0.140	2.600	1.18
	37	0.829	0.593	0.306		
		2.739	0.407	0.394	2.154	3.24
		0.817	0.583	0.297		
		2.621	0.364	0.595		
		3.292	0.054	0.108	2.157	3.47
100 μM	5	1.599	0.652	0.411		
		4.279	0.348	0.589	3.178	1.82
	25	1.372	0.754	0.525		
		3.813	0.247	0.476	2.535	0.88
	37	0.125	0.672	0.107		
		2.138	0.328	0.893	1.922	0.77

[a] All solutions contained 50 mM acetate (pH 5.0) with 5 mM Ca^{2+}.

with temperature. Examination of all the two- and three-component fits (tables 1 and 2) indicates that the intensity decays are well described by two decay times, except in the absence of Ca^{2+}, where three decay times are needed to account for the data. This can be seen from the relative decrease in χ_R^2 for the three-decay-time fits, as compared to the two-decay-time fits. In the absence of Ca^{2+} this decrease is 2.2-fold, whereas the relative χ_R^2 values decrease by only 8% in the presence of Ca^{2+}. This greater complexity in the intensity decays suggests that the environment surrounding the tyrosine residues is more heterogeneous and/or mobile in the absence of calcium.

4.2. Anisotropy decays

The anisotropy decays are of interest because they can potentially reveal the size, shape and flexibility of the calmodulin molecule. The anisotropy decays were found to be multiexponential, and for many conditions could be adequately fitted using two rotational correlation times (tables 3 and 4), as indicated by a low value of χ_R^2 and by the failure of χ_R^2 to decrease for a three-component fit. In some cases the data indicated the need for three correlation times. This is illustrated in fig. 3, which shows the two- and three-correlation-time fits for calmodulin at 5°C and pH 5, with 5 mM calcium. At present we believe the correlation times are the result of several processes. It seems probable that the shortest component (0.40 ns) is the result of both segmental mobility of the tyrosine residues and radiationless energy transfer between the two residues. The components near 2.8 and 15 ns are probably due to the combined effects of overall diffusion motions of calmodulin and internal rotations. While the analysis indicates that three correlation times are present, these values inevitably contain a good deal of uncertainty (table 4). It is perhaps simpler to consider the results from the

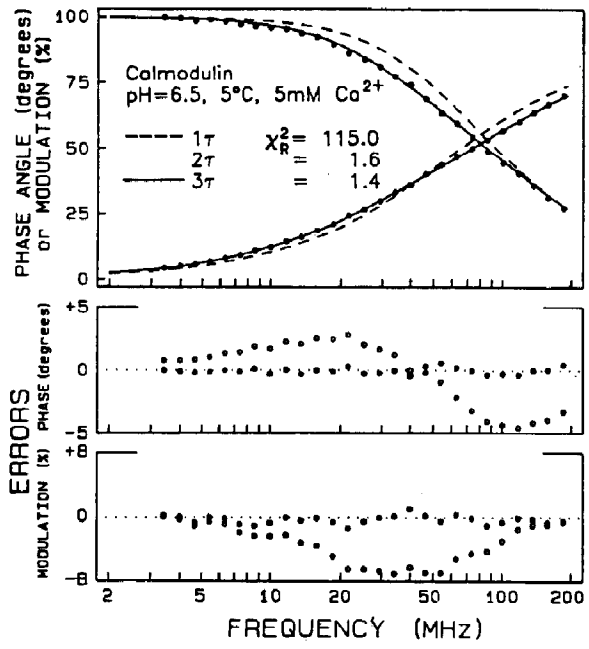

Fig. 2. Frequency-domain intensity decay of calmodulin with 5 mM Ca^{2+}, at pH 6.5 and 5° C. (———) Best two-component fit to the data (●); (------) best one-component fit. The values of χ^2_R are 115 and 1.43, respectively.

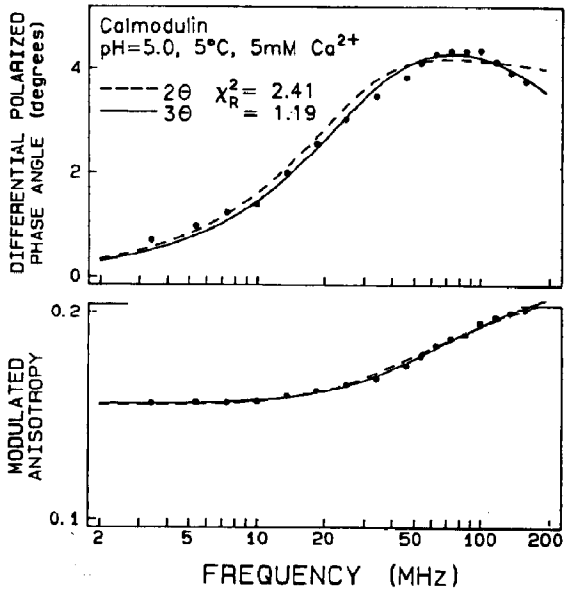

Fig. 3. Frequency-domain anisotropy decay for calmodulin tyrosine emission. The solution contained 33 μM calmodulin, 50 mM acetate (pH 5.0) and 5 mM Ca^{2+} at 5° C. (------) Best two-correlation-time fit ($\chi^2_R = 2.41$); (———) best three-correlation-time fit ($\chi^2_R = 1.19$).

two-correlation-time analysis. In this case the 0.4 ns component is probably a composite of energy transfer and segmental motions of the tyrosines and the adjacent polypeptide. The 9 ns component is comparable in magnitude to that expected for overall rotational diffusion. The possibility must be considered that a small number of discrete rotational modes is not present, but that instead a range of rotational modes and correlation times exist and that the values obtained by two- or three-component fits actually correspond to poorly defined averages. For this reason some degree of caution is advisable in interpreting the magnitude of an observed correlation time in terms of explicit structural features. However, for reasons of convenience, the results of two-component fits will be employed in comparing the effects of different experimental conditions; the cited correlation times should be regarded as apparent values.

The anisotropy decays are dependent upon the solution conditions. This is illustrated in fig. 4,

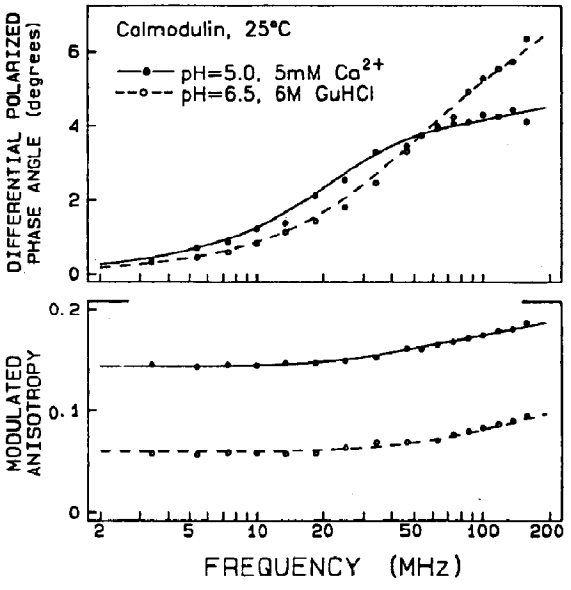

Fig. 4. Frequency-domain anisotropy data for calmodulin tyrosine fluorescence. Data are shown for 50 mM acetate with 5 mM Ca^{2+} at pH 5.0 and 25° C (●———●) and for 6 M guanidine hydrochloride, 50 mM Mops at pH 6.5 and 25° C (o- - - - -o).

Table 3

Anisotropy decays of calmodulin tyrosine fluorescence (pH 6.5)

Conditions [a]	Temperature (°C)	r_0 [b]	g_i	θ_i (ns)	θ_i^{25} (ns) [c]	$\bar{\theta}^{25}$ (ns) [d]	χ_R^2
5 mM EGTA	5	0.247	0.66	1.00 (0.02) [e]	0.54		
			0.34	19.29 (2.4)	10.41	3.95	1.25 [f]
		0.247	0.024	0.01	0.005		
			0.688	1.20	0.65		
			0.288	37.57	20.29	6.29	0.95
	37	0.247	0.25	0.12 (0.04)	0.17		
			0.75	1.49 (0.06)	2.00	1.54	0.94
		0.247	0.036	0.00	0.00		
			0.230	0.19	0.25		
			0.734	1.54	2.06	1.57	0.99
5 mM Ca^{2+}	5	0.210	0.37	1.29 (0.11)	0.70		
			0.63	10.28 (0.98)	5.55	3.79	2.86
		0.210	0.037	0.01	0.005		
			0.536	2.25	1.22		
			0.427	17.54	9.47	4.69	1.52
	37	0.210	0.65	1.44 (0.14)	1.92		
			0.35	12.31 (2.1)	16.50	6.29	1.50
		0.210	0.015	0.01	0.013		
			0.715	1.69	2.26		
			0.270	18.79	25.18	8.41	1.39
6 M GuHCl	25	0.244	0.58	0. 12	0.09		
			0.42	1.79	1.30	0.60	2.52
		0.244	0.104	0.00	0.00		
			0.503	0.18	0.13		
			0.393	1.86	1.35	0.60	2.79

[a] All solutions contained 50 mM Mops (pH 6.5) as indicated in table 1.
[b] Measured with 70% glycerol at −60 °C.
[c] Correlation times corrected to 25 °C in H_2O by multiplying by $(T/\eta)/(T/\eta)_{25°C}$, where η is the solvent viscosity.
[d] Average correlation time, corrected to 25 °C. The average was calculated using $\Sigma g_i\theta_i$.
[e] Numbers in parentheses are the uncertainties in the correlation times calculated from the diagonal elements of the error matrix [27].
[f] The uncertainties were $\delta\Delta_\omega = 0.1°$ and $\delta\Delta_\omega = 0.005$.

which shows data in the absence and presence of 6 M guanidine hydrochloride. Under denaturing conditions one finds increased phase angles at high frequencies and decreased values of the modulated anisotropies. These features are indicative of faster rotational motions of the tyrosine residues. In 6 M guanidine hydrochloride at 25 °C the apparent correlation times are 0.123 and 1.8 ns. Without guanidine hydrochloride, the correlation times are 0.25 and 7.86 ns at 25 °C (table 4).

In each case the magnitude and amplitude of the shorter correlation time were dependent upon temperature, which suggests a motional component. For instance, at pH 6.5 and 37 °C, in the absence of Ca^{2+}, the value of the shorter correlation time (124 ps) approaches that expected for a freely rotating tyrosine, whose correlation time is near 50 ps. Additionally, the rate and amplitude of the fast motion are dependent upon calcium. In the absence of calcium at 37 °C, almost all of the anisotropy decays at a rate too rapid for rotational diffusion of the intact molecule. In the presence of calcium the tyrosines retain substantial segmental freedom, but only 65% of the anisotropy appears to decay by these processes. The remainder (g_2 = 0.35) appears to be due to overall rotational diffusion.

In parallel to the behavior at pH 6.5, the fluorescence anisotropy data for pH 5.0 could be fitted in terms of two or three rotational modes.

Table 4

Anisotropy decays of calmodulin tyrosine fluorescence (pH 5.0 and 5 mM Ca^{2+})

Conditions [a]	Temperature (°C)	r_0 [b]	g_i	θ_i (ns)	θ_i^{25} (ns) [c]	$\bar{\theta}^{25}$ (ns) [d]	χ_R^2
33 μM Clm	5	0.238	0.15	0.40 (0.05) [e]	0.22		
			0.85	8.94 (0.28)	4.83	4.12	2.41 [f]
		0.238	0.072	0.02	0.01		
			0.349	2.76	1.49		
			0.579	15.43	8.33	5.43	1.19
100 μM Clm	5	0.238	0.25	0.56 (0.04)	0.30		
			0.75	12.04 (0.61)	6.50	5.03	2.99
		0.238	0.085	0.02	0.01		
			0.394	2.24	1.21		
			0.521	29.17	15.75	8.68	0.72
33 μM Clm	25	0.238	0.23	0.31 (0.03)	0.31		
			0.77	7.00 (0.25)	7.00	5.43	1.67
		0.238	0.123	0.03	0.03		
			0.444	2.24	2.24		
			0.433	16.04	16.04	7.94	0.84
100 μM Clm	25	0.238	0.23	0.25 (0.02)	0.25		
			0.77	7.86 (0.21)	7.86	6.15	2.06
		0.238	0.131	0.04	0.04		
			0.415	2.35	2.35		
			0.454	21.09	21.09	10.55	0.58
33 μM Clm	37	0.238	0.29	0.23 (0.02)	0.31		
			0.71	6.93 (0.26)	9.29	6.71	1.68
		0.238	0.061	0.00	0.00		
			0.239	0.35	0.47		
			0.700	7.16	9.59	6.82	1.84
100 μM Clm	37	0.238	0.27	0.09 (0.01)	0.11		
			0.73	6.30 (0.08)	8.45	6.19	0.54
		0.238	0.001	0.00	0.00		
			0.270	0.09	0.12		
			0.729	6.13	8.21	6.02	0.56

[a] All solutions contained 50 mM acetate (pH 5.0) as indicated in table 2.
[b] Measured in 70% glycerol at −60 °C.
[c] Correlation time corrected to 25 °C in H_2O as described in table 3.
[d] Average correlation time, corrected to 25 °C. The average was calculated using $\Sigma g_i \theta_i$.
[e] Uncertainties calculated from the nonlinear least-squares analysis [27].
[f] The uncertainties were $\delta\Delta_\omega = 0.1°$ and $\delta\Delta_\omega = 0.005$.

The more rapid of these (for a two-component fit) corresponded to a subnanosecond correlation time, while the slower rotational mode had a value of θ^{25} in the range 5–9 ns (table 4). The relative contribution of the slower mode was much greater than at pH 6.5, being over twice that of the rapid mode at 37 °C and over 3-times greater at the lower temperatures. It is clear that the immobilization of the tyrosines is substantially greater at pH 5.0 than at pH 6.5 and that some increase in mobility occurs with increasing temperature. The apparent values of the longer correlation times are roughly similar to those observed at pH 6.5 in the presence of Ca^{2+}. At pH 5.0 and 5 °C, the magnitude of the longer correlation time was significantly greater at a concentration of 100 μM than at 33 μM (table 4). This may reflect a significant degree of self-association under these conditions.

In strongly denaturing media one expects the tyrosine residues to display still greater rotational freedom. The increased motional freedom is evident from the phase angles at frequencies above 50 MHz (fig. 4). The data could be fitted to two decay times, but the longer value was only 1.8 ns (table 3). This suggests that correlation times near 1–2 ns are characteristic of random coil polypeptides.

4.3. Limiting anisotropies and energy transfer

Interpretation of the anisotropy data in terms of the dynamic and hydrodynamic properties of calmodulin is complicated by the possibility of energy transfer depolarization between the two residues. We will argue that transfer is present, but its time scale is too short to be adequately determined from the present measurements ranging to 200 MHz, and that the dominant effect of energy transfer is to reduce the value of r_0. The values of r_0 used in these calculations were obtained by direct measurements in 70% glycerol at $-70\,^{\circ}$C (table 5). Similar values were obtained for 66% propylene glycol at $-60\,^{\circ}$C (data not shown). For identical excitation and emission wavelengths the value of r_0 for *N*-acetyl-L-tyrosinamide was 0.29, which we believe is characteristic of tyrosine emission in the absence of energy transfer. The values of r_0 for calmodulin and its fragment containing both tyrosines (TR_2C) are in the range from 0.21 to 0.24. In contrast, the single tyrosine fragments (TM_1 with Tyr-99 and TM_2 with Tyr-138 show r_0 values near 0.29 at $-60\,^{\circ}$C). The decreased steady-state anisotropies for calmodulin and TR_2C indicate the presence of energy transfer depolarization. This process is not expected to be dependent upon temperature, and is known to persist at low temperatures [11]. Similar effects have been observed for synthetic polypeptides containing more than one tyrosine [20]. Since TM_1 and TM_2 each contain only a single tyrosine, transfer is absent in these cases and the limiting anisotropy has its normal value. In the case of TR_2C both tyrosines are present, so that transfer occurs and the value of r_0 is reduced. The further reduction in r_0 for Ca^{2+}-liganded calmodulin is presumably a consequence of the Ca^{2+}-induced conformational change, which reduces the separation of the tyrosines and increases the efficiency of transfer. The tertiary structures of the fragments and hence the microenvironments of Tyr-99 and Tyr-138 appear to be similar to that of native calmodulin [21].

Table 5

Limiting anisotropies of calmodulin and its fragments

Sample	Conditions	r_0 ($-60\,^{\circ}$C) [a]	r_0 (apparent) [b]
Clm	pH 6.5, 5 mM EGTA	0.247	0.241
	pH 6.5, 5 mM Ca^{2+}	0.210	0.200
	pH 5.0, 5 mM Ca^{2+}	0.238	0.221
	pH 6.5, 6 M GuHCl	0.240	0.155
TR_2C	pH 6.5, 5 mM EGTA	0.242	0.235
	pH 6.5, 5 mM Ca^{2+}	0.219	0.204
TM_1	pH 6.5, 5 mM Ca^{2+}	0.289	0.238
TM_2	pH 6.5, 5 mM Ca^{2+}	0.292	0.236

[a] All solutions were diluted with glycerol to 70% glycerol, and cooled to $-60\,^{\circ}$C.

[b] These values of r_0 were recovered from the two-correlation-time fits for $5\,^{\circ}$C, with r_0 as a variable parameter.

The anisotropy decay parameters given in tables 3 and 4 were computed using the fixed values of r_0 obtained by direct measurement in 70% glycerol at $-60\,^{\circ}$C. Since the energy transfer is expected to persist at low temperatures these parameters probably reflect dominately the motional properties of the residues, and not the component due to energy transfer. We believe the time scale of the transfer may be too rapid to be recovered from the present data, and that the process serves primarily to reduce the apparent value of r_0. It is well known that rapid components in an anisotropy decay, which are faster than the time resolution of the measurements, result in decreased apparent values for r_0 [22,23]. This suggestion is supported by an alternative analysis of the anisotropy data, in which r_0 was a

variable parameter. More specifically, the data were analyzed with $r_0 g_1$ and $r_0 g_2$ as variables in eq. 6, without restricting $\Sigma g_i = 1.0$. In most cases the apparent values of $r_0 = \Sigma_i r_0 g_i$ were comparable to the values measured at low temperature. If the time resolution were adequate to detect the faster component due to energy transfer, then the apparent values of r_0 would be expected to be near 0.29. The decreased values of the apparent values of r_0 for TM_1 and TM_2 may reflect local tyrosine motions which were not resolved by the measurements. A larger discrepancy was found for calmodulin in 6 M guanidine hydrochloride. In this case some of the rapid motions of the tyrosine residues are partially undetected, resulting in a further reduction of r_0. From these results and arguments we conclude the anisotropy decay parameters in tables 3 and 4 are dominately the result of segmental motion and rotational diffusion of the calmodulin molecule, with minor contribution from energy transfer.

5. Discussion

In agreement with the conclusions of earlier studies, these results suggest that the two tyrosine groups of calmodulin have a high degree of mobility, which is dependent upon pH, temperature, and Ca^{2+} ligation [24]. The mobility is least for the Ca^{2+}-liganded protein at pH 5.0 and at pH 6.5 and 5°C. Under these conditions the rotational motion of the tyrosines is dominated by the slower rotational mode and the most accurate values of the corresponding correlation time should be obtainable. For these conditions of maximum immobilization of the fluorophores, the values of the longer correlation time, θ_2 are in the range 5–9 ns for a two-component fit.

It is of interest to compare these values with those predicted on the assumption of an approximate hydrodynamic model. If the actual dumbbell shape of calmodulin is approximated by a prolate ellipsoid of revolution, the correlation times corresponding to the rotation of the long and short axes may be computed from the Perrin equations [25]. Because of the nonuniformity of the lateral cross-section, there is some ambiguity in the assignment of an effective axial ratio. The molecule is approx. 65 Å long and the maximum lateral dimension is approx. 20 Å, corresponding to the globular N- and C-terminal lobes. The minimum lateral dimension, corresponding to the helical cross-bridge, is in the range 6–8 Å, if an allowance is made for the side chains. Thus, the maximum and minimum values of the axial ratio are 10 and 3. The latter value is close to that computed for a prolate ellipsoid of the same molecular length and volume.

The computed correlation times for the above axial ratios and for assumed values of hydration of 0 and 0.2 are cited in table 6. The shortest correlation times are predicted for an axial ratio of 3 and zero hydration. The long correlation times that were observed are significantly less than the predicted value of θ_a for rotation of the long axis. The observed short correlation times are much less than the computed value of θ_b for rotation of the short axis. It is unlikely, therefore, that the observed correlation times correspond to rotations about the axes of the equivalent rigid ellipsoid of revolution. It is, in particular, more likely that the short correlation time reflects a localized motion of the tyrosines with respect to the overall structure.

If a hydration of 0.2 is assumed, a comparison of table 6 with the observed values of the long correlation time for conditions of maximum tyro-

Table 6

Correlation times predicted for a prolate ellipsoid of revolution [a]

Axial ratio	Hydration (g/g)	θ_a (ns)	θ_b (ns)	θ_h (ns)
3	0	10.6	5.1	7.8
5	0	21.0	5.5	10.8
10	0	60.2	5.8	14.6
3	0.2	13.4	6.5	9.9
5	0.2	26.6	7.0	13.7
10	0.2	76.3	7.3	18.5

[a] Correlation times (H_2O, 25°C) corresponding to rotation of the long axis (θ_a) and the short axis (θ_b) were computed from the Perrin equations [25], assuming a partial specific volume for calmodulin of 0.75.

[b] Harmonic mean correlation time ($\theta_h^{-1} = 1/3\ (2\theta_a^{-1} + \theta_b^{-1})$).

sine immobilization shows that the latter approach the predicted harmonic mean of θ_a and θ_b only for the limiting case of an axial ratio of 3. The relative amplitude of the more rapid rotation increases substantially with increasing temperature at both pH 6.5 and 5.0 for Ca^+-liganded calmodulin. This indicates that an increased localized flexibility is sensed by the tyrosines with increasing temperature, and suggests that some degree of thermal loosening occurs of the structures of Ca^{2+}-binding loops III and IV.

At pH 6.5 in the absence of Ca^{2+}, a substantial degree of immobilization of the tyrosines persists at 5°C. The correlation time corresponding to the slower rotational mode is, within experimental uncertainty, similar in magnitude to that found for the Ca^{2+}-liganded species, although its relative amplitude is much less. However, at 37°C, a correlation time consistent with global rotation of the protein is not observed. These results may be compared with those of Tsalkova and Privalov [26], who used differential scanning calorimetry to determine that the C-terminal lobe of apocalmodulin is thermally labile and that a substantial melting of its structure occurs in the temperature range 5–37°C.

Acknowledgements

This work was supported by grants from the National Institutes of Health (R.F.S., AM 30322) and from the National Science Foundation (J.R.L., DBM 85-02853 and DBM 85-11065).

References

1 C.B. Klee, T.H. Crouch and P.G. Richman, Annu. Rev. Biochem. 49 (1980) 489.
2 W.Y. Cheung, Science 207 (1980) 19.
3 T. Tanaka and H. Hidaka, J. Biol. Chem. 255 (1980) 11078.
4 Y.S. Babu, J.S. Sack, T.G. Greenbough, C.E. Bugg, A.R. Means and W.J. Cook, Nature 315 (1985) 37.
5 J.R. Lakowicz and B.P. Maliwal, Biophys. Chem. 21 (1985) 61.
6 J.R. Lakowicz, H. Cherek, B.P. Maliwal and E. Gratton, Biochemistry 24 (1985) 376.
7 J.R. Lakowicz, G. Laczko, H. Cherek, E. Gratton and M. Limkemann, Biophys. J. 46 (1984) 463.
8 E. Gratton, M. Limkemann, J.R. Lakowicz, B.P. Maliwal, H. Cherek, and G. Laczko, Biophys. J. 46 (1984) 479.
9 J.R. Lakowicz, G. Laczko and I. Gryczynski, Rev. Sci. Instrum. 57 (1986) 2499.
10 A.P. Demchenko, Ultraviolet spectroscopy of proteins (Springer-Verlag, New York, 1986), p. 192.
11 G. Weber, in: Fluorescence and phosphorescence analyses, ed. D.M. Hercules (Wiley, New York, 1966) p. 217.
12 D.M. Watterson, F. Sharief and T.C. Vanaman, J. Biol. Chem. 255 (1980) 962.
13 H. Brzeska, J. Szynkiewicz and W. Drabikowski, Biochem. Biophys. Res. Commun. 115 (1983) 87.
14 D. Guerini, J. Krebs and E. Carafoli, J. Biol. Chem. 259 (1984) 15172.
15 D.L. Newton, M.D. Oldewurtel, M.H. Krinks, J. Shiloach and C.B. Klee, J. Biol. Chem. 259 (1984) 4419.
16 J.R. Lakowicz, G. Laczko, I. Gryczynski and H. Cherek, J. Biol. Chem. 261 (1986) 2240.
17 R.D. Spencer and G. Weber, J. Chem. Phys. 52 (1970) 1654.
18 J.R. Alcala, E. Gratton and F.G. Prendergast, Biophys. J. 51 (1987) 587.
19 J.R. Alcala, E. Gratton and F.G. Prendergast, Biophys. J. 51 (1987) 597.
20 H. Edelhoch, R.L. Perlman and M. Wilchek, Biochemistry 7 (1968) 3893.
21 W. Drabikowski, H. Brzeska and S.Y. Venyaminov, J. Biol. Chem. 257 (1982) 11584.
22 A.J.W.G. Visser, T. Ykeme, A. van Hoek, D.J. O'Kane and J. Lee, Biochemistry 24 (1985) 1489.
23 B.P. Maliwal and J.R. Lakowicz, Biochim. Biophys. Acta 873 (1986) 161.
24 R.F. Steiner, P.K. Lambooy and H. Sternberg, Arch. Biochem. Biophys. 217 (1983) 517.
25 C.R. Cantor and P.R. Schimmel, Biophysical chemistry, vol. 2 (Freeman, San Francisco, 1980).
26 T.N. Tsalkova and P.L. Privalov, J. Mol. Biol. 181 (1985) 533.
27 P.R. Bevington, Data reduction and error analysis for the physical sciences (McGraw-Hill, New York, 1969) p. 242.